

# **CHAPTER 8**

## **SHUTTLE SPACE SUIT:**

### **FABRIC/LCVG**

### **MODEL VALIDATION**

(previously published)

J.W. Wilson  
NASA Langley Research Center  
Hampton, Virginia

J. Tweed  
Old Dominion University  
Norfolk, Virginia

C. Zeitlin  
DOE Lawrence Berkeley National Laboratory  
Berkeley, California

M.-H. Y. Kim  
College of William and Mary  
Williamsburg, Virginia

B.M. Anderson  
George Washington University  
Hampton, Virginia

F.A. Cucinotta  
NASA Johnson Space Center  
Houston, Texas

J. Ware, A.E. Persans  
ILC Dover  
Frederica, Delaware

## **ABSTRACT**

A detailed space suit computational model is being developed at the Langley Research Center for radiation exposure evaluation studies. The details of the construction of the space suit are critical to estimation of exposures and assessing the risk to the astronaut on EVA. Past evaluations of space suit shielding properties assumed the basic fabric layup (Thermal Micrometeoroid Garment, fabric restraints, and pressure envelope) and LCVG could be homogenized as a single layer overestimating the protective properties over 60 percent of the fabric area. The present space suit model represents the inhomogeneous distributions of LCVG materials (mainly the water filled cooling tubes). An experimental test is performed using a 34-MeV proton beam and high-resolution detectors to compare with model-predicted transmission factors. Some suggestions are made on possible improved construction methods to improve the space suit's protection properties.

## **INTRODUCTION**

The construction of ISS requires 1500 hours of EVA during construction and 400 hours per year in operations and maintenance. The orbit at 51.6 degrees inclination is in a highly variable radiation environment driven by solar activity. SPEs will enter this region, especially during an associated geomagnetic storm. The geomagnetic storm conditions also increase the trapped electron environment by up to four orders of magnitude; this electron enhancement can persist for several days. Although safety demands that such events be avoided if possible, work activity may not allow the astronaut to seek shelter in a timely fashion and the transmission properties of the basic suit are critical to astronaut safety. These exposures will add to the usual quiet-time exposures to trapped protons and electrons and galactic cosmic rays experienced by the astronaut.

The driving factor in this study is the need for an adequate space suit model for the estimation of exposures for mission planning and evaluation of safety during radiation field disturbance. Although there are several issues related to the protective properties of the space suit, we will address herein only the least shielded portions of the suit, which provides the basic protection of a large fraction of the body surface. In particular, the basic fabric portion of the suit mainly gives protection to the skin from the least penetrating radiation components. Other critical space suit issues will be addressed in subsequent studies. In addition, an improved understanding of the basic transmission properties of the space suit fabric components, which is a complex layup of materials, will provide a guide to improving the basic fabric design. Other critical space suit components will be addressed in subsequent studies.

It is customary in estimating the fabric transmission properties to assume the basic fabric layup is a homogenized whole of the associated materials [1,2]. In the present document, we will analyze this assumption in detail and perform experimental tests of this assumption using low-energy proton beams.

## **COMPUTATIONAL MODEL**

The types and energy distributions of particles transmitted through a shield material require the solution to the Boltzmann transport equation with appropriate boundary conditions related to the external space radiation

environment. The relevant transport equation [3] for the flux density  $\phi_j(x, \Omega, E)$  of type  $j$  particles moving in direction  $\Omega$  with energy  $E$  is given as

$$\Omega \cdot \nabla \phi_j(x, \Omega, E) = \int \sigma_{jk}(\Omega, \Omega', E, E') \phi_k(x, \Omega', E') d\Omega' dE' - \sigma_j(E) \phi_j(x, \Omega, E) \quad (1)$$

where  $\sigma_j(E)$  is the media macroscopic cross section for removal of  $j$  particles of energy  $E$ ,  $\sigma_{jk}(\Omega, \Omega', E, E')$  are the media macroscopic cross sections for various atomic and nuclear processes adding  $j$  particles of energy  $E$  in direction  $\Omega$  including spontaneous disintegration. In general, there are hundreds of particle fields  $\phi_j(x, \Omega, E)$  with several thousand cross-coupling terms  $\sigma_{jk}(\Omega, \Omega', E, E')$  through the integral in equation (1). The total cross section  $\sigma_j(E)$  with the medium for each particle type of energy  $E$  may be expanded as

$$\sigma_j(E) = \sigma_{j,at}(E) + \sigma_{j,el}(E) + \sigma_{j,r}(E) \quad (2)$$

where the first term refers to collision with atomic electrons, the second term is for elastic nuclear scattering, and the third term describes nuclear reactive processes and is ordered as  $1:10^{-5}:10^{-8}$ . This ordering allows flexibility in expanding solutions to the Boltzmann equation as a sequence of physical perturbative approximations. The atomic interactions are treated using energy moments in which the leading term is the usual continuous slowing down approximation. Special problems arise in the perturbation approach for neutrons for which the nuclear elastic process appears as the first-order perturbation and has been the recent focus of research [4,5].

Important to low-energy proton penetration are the atomic processes. Traditionally we have used the first energy moment to describe the energy loss in atomic processes and the resulting range-energy relations. More recently, the second energy moment has been added as related to range straggling [6] with added improvements resulting to the evaluations shown in **Figure 8-1**. Shown in the figure is the second moment presented as the full width at half maximum (FWHM) of the resultant energy distribution about the first energy moment seen at a depth  $x$  in aluminum for 49.1 MeV protons where  $R_0$  is the mean range. Excellent agreement is found for the second energy moment in comparison with the experiments of Tschalar and Macabee [7].

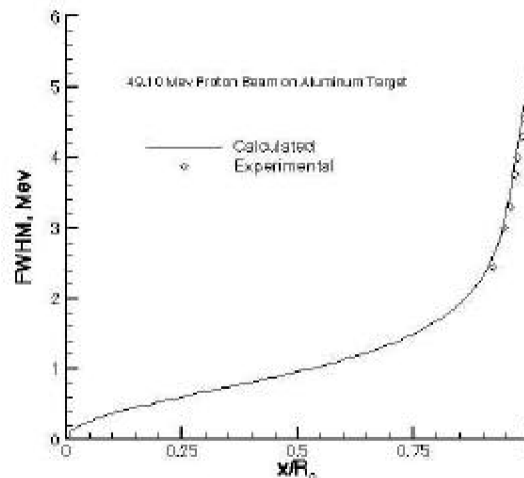


**Figure 8-1.** FWHM of 49.1 MeV protons in an aluminum target.

## SPACE SUIT FABRIC MODEL

The Shuttle space suit is manufactured by ILC Dover for use in the space program. The basic components are shown in **Figure 8-2**. Not shown in the figure is the life support system held mainly in a backpack attached to the HUT. We are mainly concerned herein with the Arm assembly and Lower Torso Assembly (LTA) consisting mainly of fabric and the LCVG consisting of fabric and the water filled cooling tubes. The basic layout of the fabric and LCVG are shown in **Figure 8-3**.

The most easily penetrated portion of the space suit is covered only by the fabric (Arm Assembly and LTA) and the LCVG. This is of greatest importance when the environment contains low energy particles with limited penetration power. Most environmental components contain such particles, and these are often the most intense component. They are only of concern for tissues which are poorly shielded and not of concern within a space vehicle assembly such as the Shuttle or ISS or for organs deep within the body. The basal layer of the skin is somewhat sensitive to radiation and therefore of concern in a lightly shielded space suit in an intense and low-energy environment.

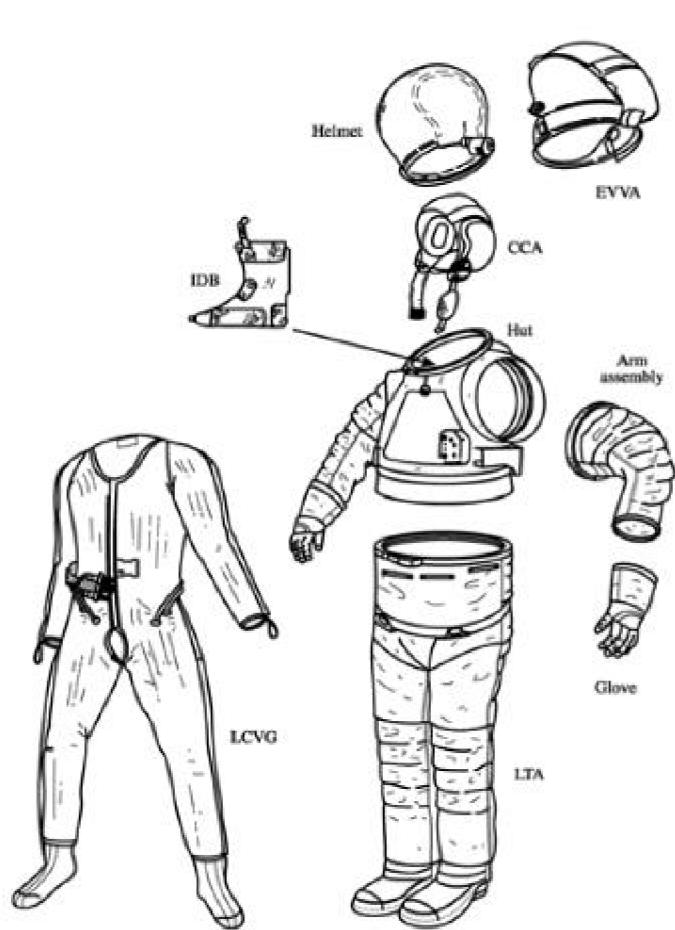


**Figure 8-2.** Basic components of the Shuttle space suit.

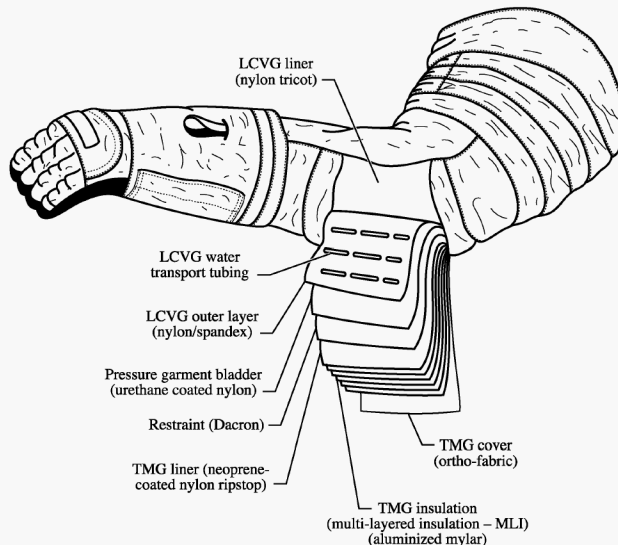


**Figure 8-3.** Cross section of material layup.

The material layup for the fabric including the inner LCVG is given in **Table 8-1**. The outer fabric layer, the Thermal Micrometeoroid Garment (TMG), is composed of the OrthoFabric, five layers of Reinforced Aluminized Mylar for thermal insulation and Neoprene Coated Nylon Ripstop. Below the TMG is the Dacron® pressure restraint. This is followed by the Urethane Coated Nylon (pressure bladder) and the LCVG of a multifilament Nylon/Spandex knit which contains the ethylvinyl-acetate tubes filled with water.

**Table 8-1.** Material Layup of the Space Suit Fabric and Water Filled Tube [1,8]

Material	Areal density, g/cm <sup>2</sup>
Orthofabric-Teflon/Nomex/Kevlar	0.049
Reinforced Aluminized Mylar	0.014
Neoprene Coated Ripstop	0.028
Dacron® Polyester	0.021
Urethane Coated nylon Ripstop	0.014
Nylon/Spandex/water/ethylvinylacetate	0.154

In past calculations [1], the materials in **Table 8-1** were described by equivalent amounts of aluminum by scaling with the ratio of range of a 50 MeV proton in aluminum to the range in the specific material and calculations made for penetration in the equivalent aluminum. There are three concerns with this approach: the equivalent aluminum scale factor depends on the proton energy yet the assumed equivalency at 50 MeV is not accurate for minimum penetration particles; the water filled tubes cover only 40 percent of the surface area and the homogenization with the Spandex over-estimates the protection properties of the fabric (with homogenized tube) over 60 percent of the area; and, many components of the fabric layup are inhomogeneous structures and may not be well represented by an average areal density.

The surest way to represent the actual fabric/tube transmission properties is to remove these defects by representing the water filled tube geometry specifically, transporting through actual material layers as opposed to assuming equivalent aluminum, and performing penetration test to test models of the inhomogeneities within the remaining fabric. These tasks are performed in the present study and the fabric transmission properties are represented as an analytical model with good agreement with low-energy proton transmission testing. The improved understanding of the fabric transmission properties will allow redesign considerations to improve the space suit radiation safety. The basic penetration test is shown schematically in **Figure 8-4**. The test is in principle quite simple; a low-energy proton beam is incident from the left on a swatch of the space suit and water filled tubes as shown. The arrangement of the experimental setup is shown in **Figure 8-5** as used in the present testing. A reasonably uniform beam of approximately 34.5 MeV protons enters the Lexan collimator from the left and is monitored by a 3mm thick silicon detector (d3mm1). The transmitted spectrum through d3mm1 was measured in a “target out” test. The monitored beam passes through the target station and analyzed by a set of position sensitive detectors (PSD1X&Y) with total remaining energy detected by the 5-mm silicon detector (d5mm1).

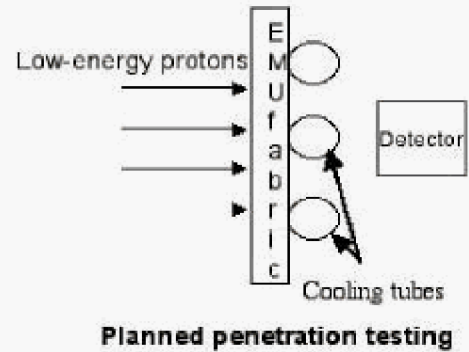


**Figure 8-4.** Basic experimental set up.

The test is in principle quite simple; a low-energy proton beam is incident from the left on a swatch of the space suit and water filled tubes as shown. The arrangement of the experimental setup is shown in **Figure 8-5** as used in the present testing. A reasonably uniform beam of approximately 34.5 MeV protons enters the Lexan collimator from the left and is monitored by a 3mm thick silicon detector (d3mm1). The transmitted spectrum through d3mm1 was measured in a “target out” test. The monitored beam passes through the target station and analyzed by a set of position sensitive detectors (PSD1X&Y) with total remaining energy detected by the 5-mm silicon detector (d5mm1).

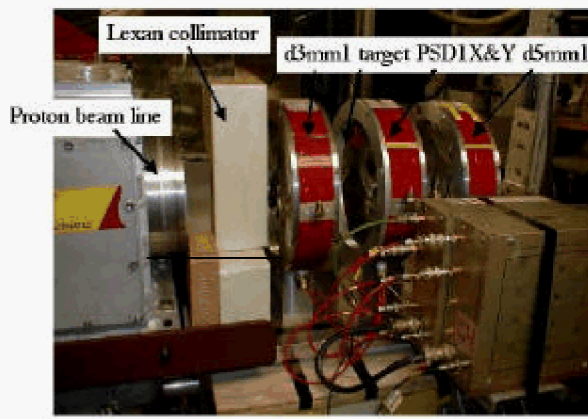


**Figure 8-5.** Proton beamline used at the LBNL 88” cyclotron.

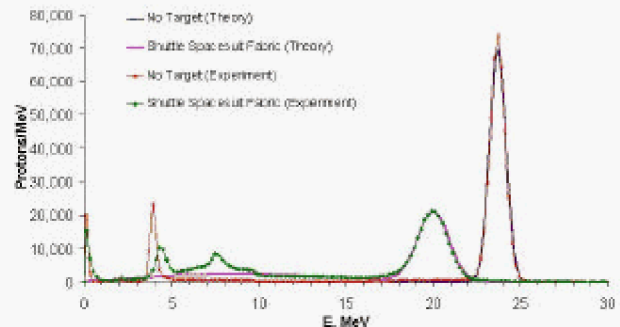


**Figure 8-6.** Experimental and analysis results.

## RESULTS AND IMPLICATIONS

The beam was first analyzed without the target in place with results (no target) appearing as the near normal distribution of particles at the far right in **Figure 8-6**. The computational model was fit to the beam parameters before the d3mm1 and found to be of 34.54 MeV with a standard deviation of 0.27 MeV resulting in the  $23.68 \pm 0.46$  MeV beam incident on the target shown in the figure. The additional broadening of the energy spectrum is due to

straggling in the d3mm1 monitor. The results of the analysis are shown in comparison to the experimental estimate of the beam properties at the target. There is an added spectral feature near 4 MeV in the experimental data believed to be due to multiple scattering effects in the collimator.

The beam transmitted through the target is shown also in the figure. The spectral feature at  $19.94 \pm 0.967$  MeV results from the transmission through the fabric without a tube in the proton path. The increased width of this peak relative to the beam before the target results from straggling effects in the fabric and the non-uniformity of some of the fabric components. The fabric is best fit as a normal distribution of material of mean thickness of  $0.161 \pm 0.03$  g cm<sup>-2</sup> of material. The mean areal density of the fabric (without the cooling tubes) is measured to be  $0.185$  g cm<sup>-2</sup>. The height of the transmitted peak is critically dependent on the size of the tube (tube diameter is 4 mm) and tube spacing (1 per centimeter). In the model, the water filled tube was assumed to be a homogeneous mixture of appropriate mass of water and ethylvinylacetate. The experiment indicates that the improved penetration properties of the water may be apparent in the data as the experimental transmitted spectral feature near 7 MeV may be due to water in the tube. Hence, some added detail for the model is required.

## FUTURE ACTIVITY

The next step in the analysis will be to model the tube to better understand the lowest energy transmission of this complex system. Additional experiments will be performed to better understand the source of the non-uniformity of the fabric components. This will be accomplished by noting that the penetration properties of the fabric components are near that of polycarbonate. The nonuniform elements (e.g., spandex) will be modeled by an equivalent sheet of uniform polycarbonate and the transmitted spectrum will be determined and analyzed. This should provide a reasonable model of the space suit fabric and cooling tubes for use in estimating astronaut exposures. Finally it would be desirable to study the electron transmission characteristics for which the basic physical description of the fabric should be similar. An appropriate electron beam for experimental testing is being investigated.

Secondly, upon complete understanding of the current space suit transmission properties we can improve estimates of the astronaut exposures in space activity [9]. In addition, this understanding of the performance of the fabric layup elements and experimental testing procedures will allow evaluation of alternative space suit designs.

The next least protected critical organ is the lens of the eyes. They are protected mainly by the helmet components. Plans for testing the helmet component transmission properties are in progress.

## CONCLUSION

Considerable progress was made in understanding the basic transmission properties of the space suit fabric as it is now used in the space program. Additional detail is required to adequately model the proton transmission properties of the LCGV cooling tubes. It is desirable to also study the electron transmission properties to insure that a consistent picture of the space suit fabric is obtained. The basic fabric model as outlined is being integrated into a space suit model for estimates of astronaut exposures during future missions.

## REFERENCES

1. Kosmos J.J., Nachtwey D.S., Hardy A. JSC/CTSD-SS-241, 1-24-1989.
2. Wilson J. W. et al. NASA CP 3360, 1997.
3. Wilson, J. W. et al., Transport Methods and Interactions for Space Radiations. NASA Reference Publication, RP-1257, 1991
4. Heinbockel, J. H. et al. An Improved Neutron Transport Algorithm for Space Radiation. NASA TP-2000-209865, 2000.
5. Cloudsley, M. S. et al., A comparison of the multigroup and collocation methods for solving the low energy neutron Boltzmann equation. To be published Cana. J. Phys. 78: 45-56, 2000.
6. Wilson J.W., Tai H.A. NASA 2000-209864, 2000.
7. Tschalar C., Maccabee, H. D. Phys. Rev. B 1: 2863-2869, 1970.
8. Ross A.J. et al. NASA CP 3360, 1997.
9. Anderson B. M. et al. SAE 01ICES-147, 2001.

## CONTACT

The communicating author email address is:

John.W.Wilson@LaRC.NASA.GOV